

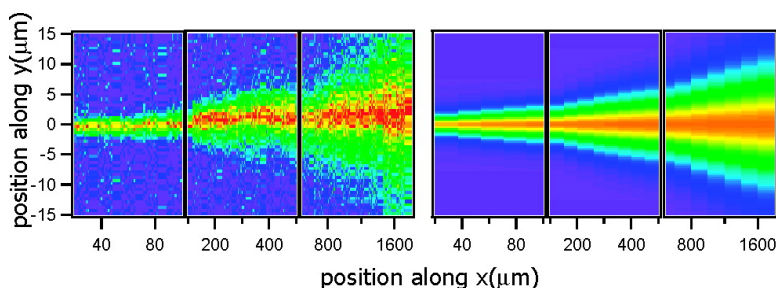
Communication

In Situ Quantitative Measurement of Concentration Profiles in a Microreactor with Submicron Resolution Using Multiplex CARS Microscopy

Dawn Schafer, Jeff A. Squier, Jan van Maarseveen, Daniel Bonn, Mischa Bonn, and Michiel Müller

J. Am. Chem. Soc., **2008**, 130 (35), 11592-11593 • DOI: 10.1021/ja804158n • Publication Date (Web): 08 August 2008

Downloaded from <http://pubs.acs.org> on February 8, 2009



More About This Article

Additional resources and features associated with this article are available within the HTML version:

- Supporting Information
- Access to high resolution figures
- Links to articles and content related to this article
- Copyright permission to reproduce figures and/or text from this article

[View the Full Text HTML](#)

In Situ Quantitative Measurement of Concentration Profiles in a Microreactor with Submicron Resolution Using Multiplex CARS Microscopy

Dawn Schafer,[†] Jeff A. Squier,[†] Jan van Maarseveen,[‡] Daniel Bonn,[‡] Mischa Bonn,^{*,§} and Michiel Müller[‡]

Department of Physics, Colorado School of Mines, 1523 Illinois Street, Golden, Colorado 80401, University of Amsterdam, Nieuwe Achtergracht 129, 1018 WS Amsterdam, The Netherlands, and FOM Institute for Atomic and Molecular Physics, Kruislaan 407, 1098 SJ, Amsterdam, The Netherlands

Received June 2, 2008; E-mail: bonn@amolf.nl

Microfluidic devices present an increasingly important platform for areas as diverse as catalysis, biotechnology, and analytical and combinatorial chemistry.¹ Microfluidic devices are ideal reaction vessels and enable continuous processing, with unprecedented control over reactants and their mutual contact. It has been a challenge to follow chemical transformations in microfluidic devices in real space and real time. The small sample volumes associated with microfluidics dictate that highly sensitive, high-resolution techniques are required for real-space characterization of chemical species within the device. As a result, a number of microscopic methods based on spectroscopy have been applied for on-chip analysis. Optical methods, such as fluorescence-based microscopies, are attractive owing to their potentially high (single-molecule) sensitivity but are not inherently chemically specific.^{2,3} Raman-based methods are therefore very attractive, as chemical transformations in the microfluidic devices induce vibrational changes that are readily detectable. Indeed, confocal Raman microscopy (see, e.g., refs 3–8) and surface-enhanced resonant Raman scattering⁹ have provided important insights into diffusion and reactions in microfluidic devices. However, the relatively small Raman cross sections indicate, relative to UV/vis methods, the sensitivity is reduced and hence high concentrations and long data acquisition times are required, ranging from seconds to minutes. The effective cross sections can be increased using surface-enhanced Raman techniques, but these inherently rely on inhomogeneous electromagnetic field amplifications, so that the signal is not linear in the local concentration. As an alternative Raman technique, Coherent Anti-Stokes Raman Scattering provides much improved sensitivity over conventional Raman (by a factor of typically 10³) and quantitative species determination. CARS has been highly successfully used in (cellular) imaging^{10–12} and microfluidic cytometry.¹³

We present here multiplex Coherent Anti-Stokes Raman Scattering (CARS) spectroscopy for monitoring chemical processes in a microfluidic device by using a very rapid acid–base reaction as a model reaction. We demonstrate label-free, chemically specific, quantitative determination of local concentrations of reactants and products, with 3D submicron spatial resolution (400 nm in *x* and *y* directions; 1.5 μm in *z* direction). At any given position within the device, the total measurement time required to record a full spectrum across 400 cm⁻¹ is 20 ms, allowing local concentrations to be determined with ~10 mM accuracy. This unprecedented sensitivity and speed of this quantitative, in situ method opens new avenues for monitoring reactions in microfluidic environments.

Details of the CARS setup can be found in the Supporting Information. The transformation of 300 mM solutions of acetic acid

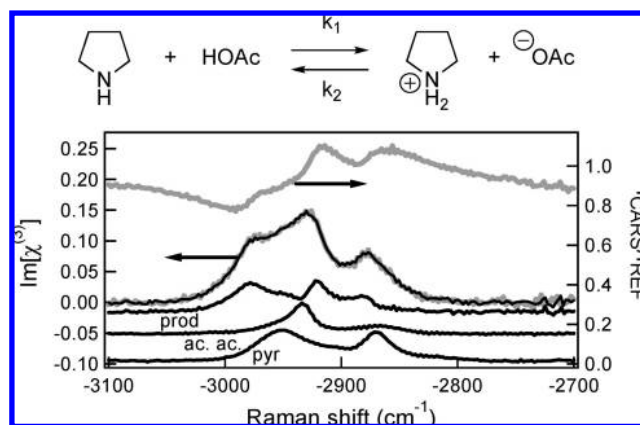


Figure 1. Upper: proton transfer reaction between pyrrolidine (pyr) and acetic acid (ac. ac.) investigated in the microfluidic device to form the product (prod, a salt). Lower panel: Raw CARS data (gray, upper trace), normalized to the reference signal, measured 240 μm downstream from the mixing junction, at the center and a depth of 9 μm. Lower traces: Retrieved Raman response (gray line) with the result of the analysis described in the text (black line), which shows that, at this position (center of the flow), the fractions of reactants and product amount to roughly 1/3 each. Lower three traces: Inferred Raman response of the two reactants and the product used in the quantitative analysis of local concentrations.

(CH₃COOH) and pyrrolidine (C₄H₉N) in deuterated 1,4-dioxane into their conjugate base and acid, respectively, is shown in Figure 1. The reaction was followed in a microfluidic device characterized by a Y-shaped, 2-inlet mixing junction (Miconit, Enschede, NL) with a depth and width of, respectively, 23 and 46 μm. Fluid flow was typically 5 × 10⁻³ mL/min. This particular reaction was chosen to demonstrate the sensitivity of the approach: we demonstrate that the transfer of a proton from oxygen to nitrogen can be followed through the vibrations of the unaltered C–H groups around 2900 cm⁻¹. Raw CARS spectra are determined by the third-order nonlinear susceptibility χ⁽³⁾, a complex sum of resonant and nonresonant contributions. The interference between these contributions makes quantitative analysis of CARS spectra very challenging. However, it has been shown that the imaginary part of the resonant χ⁽³⁾, Im[χ⁽³⁾], is, under specific experimental conditions, equivalent to the spontaneous Raman signal and thus provides quantitative information on molecular concentrations.¹⁴ To retrieve Im[χ⁽³⁾], the phase and amplitude of χ⁽³⁾ are determined using the Maximum Entropy Method.¹⁴ CARS spectra of the pure reactant solutions (recorded in the inlet channels) were used to calibrate the Raman response. The resulting Im[χ⁽³⁾] spectra shown in Figure 1 were indistinguishable from spontaneous Raman measurements on the same reactant solutions in bulk. For the product spectrum, we did not distinguish between the conjugate acid and base spectra. The

[†] Colorado School of Mines.

[‡] University of Amsterdam.

[§] FOM Institute for Atomic and Molecular Physics.

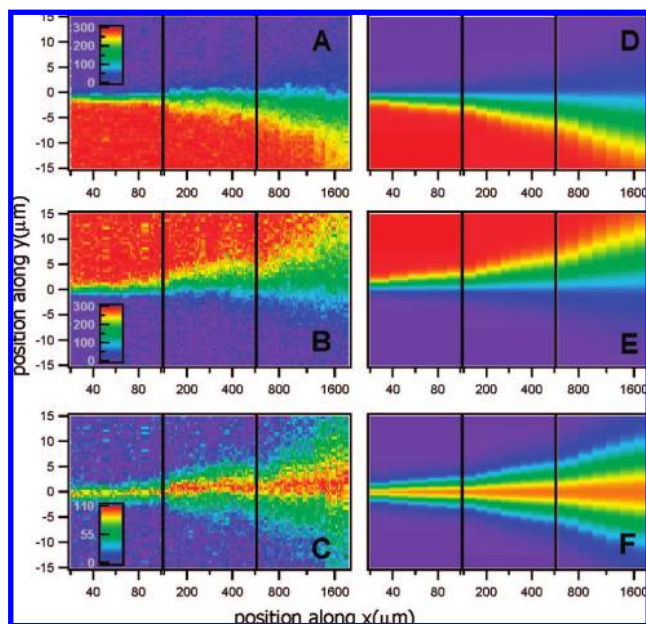


Figure 2. Concentration profiles of pyrrolidine (A), acetic acid (B), and the reaction product (salt) (C) within the microfluidic device. Panels (D), (E), and (F) provide the corresponding results of the numerical simulations described in the text. The full color scale represents, for (A, B, D, E), a concentration variation from 0 to 300 mM and, for (C) and (F), from 0 to 110 mM. Note the different tick increments along the x -scale for each of the three panels for each figure; $y = 0$ denotes the center of the channel.

product $\text{Im}[\chi^{(3)}]$ spectrum measured downstream in the center of the microfluidic device (Figure 1) matched Raman measurements for a bulk solution at equilibrium.

To characterize the evolution from reactants to product within the microfluidic device, the Raman spectrum was determined for every (x, y) position at a depth of $z = 9 \mu\text{m}$. The upper trace in Figure 1 shows a typical normalized spectrum (raw CARS data divided by reference spectrum in glass) for a postmixing position. The lower traces show the inferred $\text{Im}[\chi^{(3)}]$ spectrum, along with the retrieved Raman spectrum (gray lines). The Raman spectrum is a linear sum of the spectral contributions from each constituent species (black line). The weights of each spectral contributions, shown as the lower three traces, are fit parameters, which directly reveal the local concentration of the three components. This procedure allows us to determine local concentration maps for the central $30 \mu\text{m}$ of the channel at various distances from the mixing point (total data collection time 20 min) as shown in Figure 2 for the two reactants (Figure 2A, B) and the product (Figure 2C). The total product yield as a function of the downstream position (Figure 3) scales linearly with the square root of the downstream position, indicating that diffusion is rate limiting.

Indeed, the data are readily modeled using a reaction-diffusion model.¹⁵ As input we need (i) the diffusion coefficients of the reactants, which were determined independently in an experiment with only one of the two reactants present ($D = 7 \times 10^{-6} \text{ cm}^2/\text{s}$ for both reactants) and (ii) the overall reaction constant $K = k_1/k_2 = 7.8$, which was determined from bulk equilibrium measurements. The results of numerical simulations are shown in Figures 2D–F and 3. The agreement with the data is excellent in the limit that k_1 and k_2 are very large (i.e., diffusion limited reaction). The only adjustable parameter is the diffusion coefficient of the

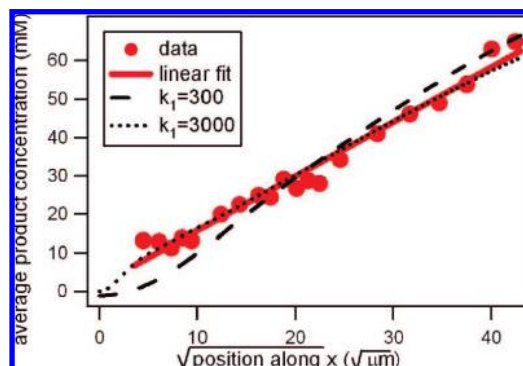


Figure 3. Measured average product concentration in the microfluidic device as a function of downstream coordinate x (circles) along with a least-squares linear fit (solid line) and two simulation results for different rate constants (dashed and dotted lines). The fast initial increase in product is caused by the rapid formation of product at the junction.

product, to which the results are not very sensitive, set at $D = 5 \times 10^{-6} \text{ cm}^2/\text{s}$. A comparison between the simulated and measured rate of product formation (Figure 3) sets a lower limit on k_1 of $300 \text{ L}(\text{mol s})^{-1}$.

These results demonstrate the power of CARS spectroscopy for rapid, local determination of reactant and product concentrations and, thereby, the local reaction efficiency. The successful implementation shown here for a reaction characterized by relatively small changes in chemical structure illustrates that the approach is widely applicable. As a quantitative characterization tool, CARS is particularly appealing for systems where effects of inhomogeneities may be large, such as a supported catalyst integrated in microfluidic environments. Rapid in situ quantification of these effects may lead to significant improvement in device design. Furthermore, the ability to perform quantitative measurements on ms time scales opens the way to perform real-time online feedback to optimize reaction parameters, providing an attractive alternative to existing combinatorial approaches.

Supporting Information Available: Details on the experimental setup, data analysis, and modeling. This material is available free of charge via the Internet at <http://pubs.acs.org>.

References

- (1) deMello, A. J. *Nature* **2006**, *442*, 394–402.
- (2) Magennis, S. W.; Graham, E. M.; Jones, A. C. *Angew. Chem., Int. Ed.* **2005**, *44*, 6512–16.
- (3) Park, T.; Lee, M.; Choo, J.; Kim, Y.; Lee, E. K.; Kim, D. J.; Lee, S.-H. *Appl. Spectrosc.* **2004**, *58*, 1172–79.
- (4) Fletcher, P.; Haswell, S.; Zhang, X. *Electrophoresis* **2003**, *24*, 3239–45.
- (5) Lee, M.; Lee, J.-P.; Rhee, H.; Choo, J.; Chai, Y. G.; Lee, E. K.; Raman, J. *Spectroscopy* **2003**, *34*, 737–42.
- (6) Salmon, J.-B.; Ajdari, A.; Tabeling, P.; Servant, L.; Talaga, D.; Joanicot, M. *Appl. Phys. Lett.* **2005**, *86*, 094106.
- (7) Araki, T.; Ueno, K.; Misawa, H.; Kitamura, N. *Anal. Sci.* **2006**, *22*, 1283–89.
- (8) Barnes, S. E.; Cygan, Z. T.; Yates, J. K.; Beers, K. L.; Amis, E. J. *Analyst* **2006**, *131*, 1027–33.
- (9) Zhang, X.; Yin, H.; Cooper, J. M.; Haswell, S. J. *Anal. Bioanal. Chem.* **2008**, *390*, 833–40.
- (10) Cheng, J. X.; Xie, X. S. *J. Phys. Chem. B* **2004**, *108*, 827–40.
- (11) Li, L.; Cheng, J. X. *J. Phys. Chem. B* **2008**, *112*, 1576–79.
- (12) Evans, C. L.; Xu, X. Y.; Kesari, S.; Xie, X. S.; Wong, S. T. C.; Young, G. S. *Opt. Express* **2007**, *15*, 12076–87.
- (13) Wang, H. W.; Bao, N.; Le, T. T.; Lu, C.; Cheng, J. X. *Opt. Express* **2008**, *16*, 5782–89.
- (14) Vartiainen, E. M.; Rinia, H. A.; Müller, M.; Bonn, M. *Opt. Express* **2006**, *14*, 3622–30.
- (15) Salmon, J.-B.; Ajdari, A. *J. Appl. Phys.* **2007**, *101*, 074902.

JA804158N